

Miniaturization of a Circular Polarized Antenna using Ferrite Materials

E. Arnaud¹, L. Huitema¹, R. Chantalat², A. Bellion³, T. Monediere¹

¹ Xlim UMR 7252 CNRS/ Université de Limoges, 123 Avenue Albert Thomas, 87060 Limoges Cedex, France, eric.arnaud@xlim.fr, laure.huitema@xlim.fr

² CISTEME, 12 rue Gémini 87069 Limoges Cedex, France

³ Centre National d'Études Spatiales (CNES), 18 Avenue Edouard Belin, 31400 Toulouse, France

Abstract— A miniature antenna with an optimized circular polarization is presented in this paper. It uses the specific behavior of the electromagnetic wave's propagation in ferrite materials to create the nonreciprocity phenomenon and thus a natural circular polarization. Moreover, both the high permittivity and permeability of such a material imply that the antenna is miniaturized. In this framework, a magnetostatic and electromagnetic co-simulation of a circular polarized ferrite patch antenna working at 2 GHz is presented with reduced dimensions of $\lambda_0/8.5 \times \lambda_0/8.5 \times \lambda_0/37$ at 2 GHz.

Index Terms—Miniature antenna, circular polarization, ferrite material.

I. INTRODUCTION

Wireless sensor networks for IoT, Car2X communications as well as satellite positioning and communicating devices require miniature antennas with a circular polarization. It is a real challenge to combine these two properties since miniature antennas often have either a linear polarization [1] or for ultra-miniature antennas with bending structures a “random” polarization (neither linear nor circular) [2]. Circular polarized antennas need for a feeding network which can include phase shifters, couplers and SMD components. It can be therefore too much cumbersome when a miniature device is aimed. In this framework, antennas based on ferrite materials can be a good alternative since this material owns specific magnetic properties in high frequencies. Indeed, a phenomenological description of circular ferrite resonators shows two counter-rotating modes within the resonator when they are biased with an external DC magnetic field [3]. This main property of ferrites has been largely used for developing RF circulators [4-5]. Despite the diversity of theoretical analyzes related to ferrite circulators, only few papers are presenting antennas based on ferrites. Among these papers, N. Das showed in [6] that using a ferrite substrate for a patch antenna can lead to the reduction of its global dimensions while improving both its realized gain and its impedance bandwidth. In [7], authors presented how to take advantage of the non-reciprocity phenomena of ferrites by obtaining a circular polarized patch antenna by using only one excitation probe. Some reconfigurable solutions, i.e. beam and frequency tuning, based on the modification of the applied DC magnetic fields have been presented in [8-9].

All these papers are based on theoretical models without taking into account the real applied DC magnetic field and are limited to consider it as uniform within the ferrite. In this paper, we will present the magnetostatic and electromagnetic co-simulation of a ferrite patch antenna working at 2 GHz. This antenna exhibits a circular polarization thanks to the use of a permanent magnet integrated within our co-simulation methodology. Moreover, thanks to the ferrite permittivity and the permeability profiles, which will be describe in this paper, the antenna dimensions are reduced. The next part will present general properties of ferrites in high frequencies and show their different operation modes. The part III will detail the simulation of an antenna working in the strong field area followed by the case in the weak field area. Finally, the strong field case is chosen to be detailed in part IV since this antenna presents highly reduced sizes while having good performances in terms of circular polarization and gain.

II. GENERAL PROPERTIES OF A PATCH ANTENNA DEVELOPED ON A FERRITE MATERIAL

The non-reciprocity phenomenon of a ferrite material is coming from its permeability tensor when it is biased by a magnetic field H_0 . For a biasing magnetic field enough to saturate the ferrite along the z axis, this permeability tensor is given in high frequency by the equation (1) [10].

$$\mu = \mu_0 \bar{\bar{\mu}}_r = \mu_0 \begin{bmatrix} \mu & -j\kappa & 0 \\ j\kappa & \mu & 0 \\ 0 & 0 & 1 \end{bmatrix} \quad (1)$$

where: $\mu = 1 + \frac{\omega_m \omega_0}{\omega_0^2 - \omega^2}$, $\kappa = \frac{\omega_m \omega}{\omega_0^2 - \omega^2}$, $\omega_0 = \gamma \mu_0 H_1 + j\omega\alpha$ and $\omega_m = \gamma \mu_0 M_s$

Therefore, both μ and κ are depending on the internal field in the ferrite material H_1 , the saturation magnetization M_s and the frequency f . When plotting both the real and the imaginary parts of μ , i.e. μ' and μ'' respectively, it appears a resonance called gyromagnetic resonance. Its resonance frequency equals $1.4 G_{eff}$ with G_{eff} the Lande factor. Around this resonance frequency, magnetic losses (proportional to μ'') are too high and for frequencies just above the gyromagnetic

resonance, the effective permeability of ferrite defined as $\mu_{eff} = \mu^2 - \kappa^2/\mu$ is becoming negative. Thus, the ferrite material is not usable on these frequency bands and these areas are depicted on Fig.1.

As long as antennas operate outside from these zones, two distinct operation modes are discussed: below and above the gyromagnetic resonance.

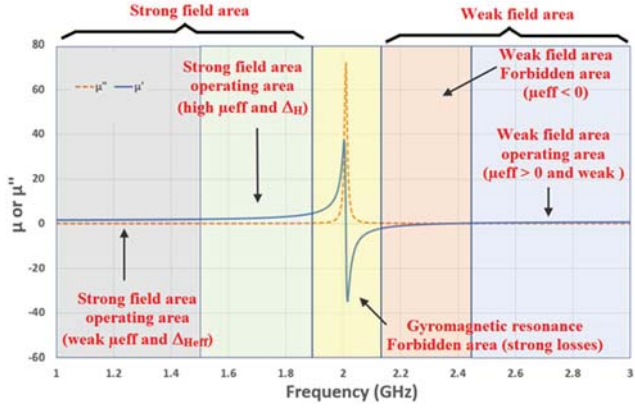


Fig. 1. Real and Imaginary parts evolution of μ versus frequency according Polder's tensor

As the gyromagnetic resonance frequency is directly depending on the internal magnetic field in the ferrite material, below and above the gyromagnetic resonance areas are respectively called strong and weak field areas. The choice of the ferrite, particularly its saturation magnetization $4\pi M_s$ (Gauss) and its relative resonance line width ΔH_{eff} (Oe), is linked to these working modes. Indeed, a ferrite with a low saturation magnetization is selected for a weak field operation while a ferrite with a low ΔH_{eff} is preferred for the strong field operation. In this framework, two kinds of ferrites have been selected and their properties are summarized in Table I.

TABLE I. FERRITE CHARACTERISTICS

Ferrite from Exxelia Temex ceramics [11]	Y36	Y208
Saturation magnetization $4\pi M_s$ (Gauss)	290	800
Relative resonance line width ΔH_{eff} (Oe)	4	2
Resonance line width ΔH (Oe)	25	10
Relative permittivity (ϵ_r)	14	14.1
Loss tangent ($\tan\delta$)	0.0002	0.0002
Selected operation mode	Weak field	Strong field
Lande factor G_{eff}	2.01	2.01

With these characteristics, we can determine the internal magnetic field to apply on each ferrite in order that the operating area is the antenna working frequency band, i.e. 2GHz. In Fig. 2, the real and the imaginary parts of μ , i.e. μ'

and μ'' are plotted for internal fields in the ferrite materials equal to 300 Oe and 900 Oe respectively.

Therefore, operating areas for the two selected ferrites are the same and around 2GHz. The next part will present the development of a patch antenna for these two cases.

III. ANTENNA DEVELOPMENT

The antenna development has been done in two steps. The first one is considering the ferrite substrate with a uniform internal magnetic field while the second step is using the magnetostatic and electromagnetic co-simulation.

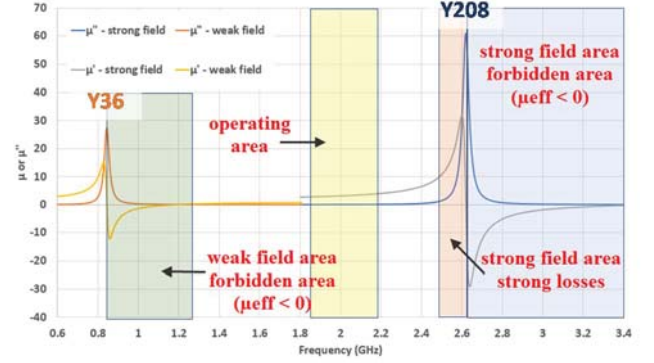


Fig. 2. Real and Imaginary parts evolution of μ for the Y36 with $H_i=300$ Oe and the Y208 with $H_i=900$ Oe

A. Antenna within a uniform magnetic field

The proposed design is depicted in Fig. 3. As a classical patch antenna, it is composed by two metallizations etched on each face of a substrate. In this case, the substrate is a ferrite material for which the Polder tensor defined in equation (1) is used within the simulation. The lower metallic plate acts as a ground plane of 50mm x 50mm and the upper metallic plate constitutes the antenna top hat, which is a square of 'a' side length. This antenna is fed by a coaxial probe which is connected to the top hat through the ground plane and the ferrite substrate.

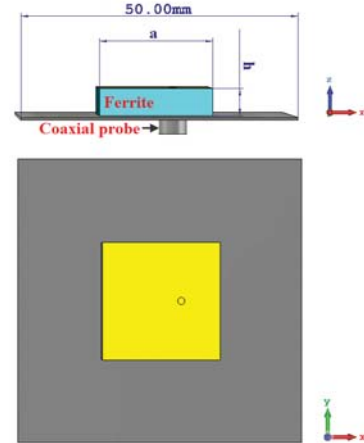


Fig. 3. Antenna design

Since the resonance frequency of such an antenna is proportional to $\frac{1}{\sqrt{\epsilon_r \mu_{eff}}}$, antenna top hat dimensions are differing according to the operation modes, i.e. weak or strong field. Table II is listing antennas' dimensions for each working case with the real part value of the permeability μ' at 2 GHz.

TABLE II. COMPARISON OF THE ANTENNA CHARACTERISTICS

	a (mm)	ferrite thickness h (mm)	μ' at 2 GHz
Weak field (Y36-300 Oe)	20.6 mm ($\lambda_0/7$) [*]	5mm ($\lambda_0/30$) [*]	0.8
Strong field (Y208-900 Oe)	15.6 mm ($\lambda_0/10$) [*]	6 mm ($\lambda_0/25$) [*]	3.3
* λ_0 is calculated at 2GHz			

$|S_{11}|$ parameters are plotted for both the strong and the weak fields in Fig. 4. The weak field case is using the Y36 ferrite with an internal magnetic field H_i of 300 Oe and the strong field uses the Y208 ferrite with $H_i = 900$ Oe. With a magnetic field oriented according to the positive z-axis, the antenna has a right-handed circular polarization (RHCP) for the strong field case while it has a left-handed circular polarization (LHCP) for the weak field case around 2 GHz.

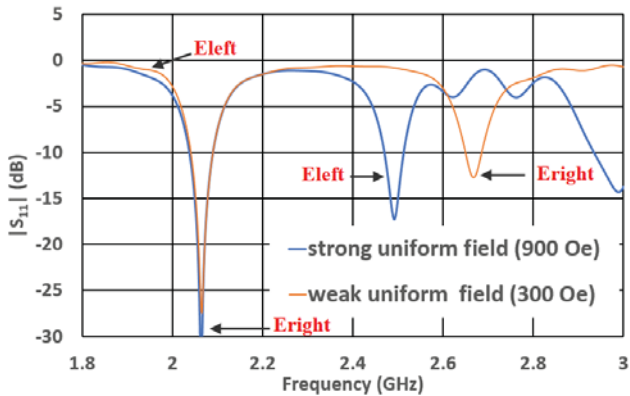


Fig. 4. $|S_{11}|$ parameters for the strong field case and the weak field case

For the strong field case, the impedance bandwidth is equal to 2.6% while it equals 2.5% for the weak field case. It is thus a little higher when the antenna has a strong field operation due to the higher value of μ' . Indeed, Hansen and Burke [12] have expressed the zero-order impedance bandwidth of a patch antenna printed on a H-thick material by the equation (2):

$$BW = \frac{96 \sqrt{\epsilon_r} \cdot \frac{H}{\lambda_0}}{\sqrt{2} (4 + 17 \sqrt{\epsilon_r \mu'})} \quad (2)$$

Therefore, for the strong field case, the antenna dimensions are highly reduced while having a better impedance bandwidth.

Losses are also investigated and the Fig. 5 is comparing total losses and magnetic and dielectric losses for the two cases. Magnetic losses (proportional to μ'') are depending on the position of the antenna working frequency (2GHz) with the gyromagnetic resonance frequency. The closer they are, the higher the losses are. However, the chosen Y208 ferrite to work in the strong field has been selected to present lower losses than the Y36. It implies a total losses difference between the two weak and the strong fields of only 0.4dB.

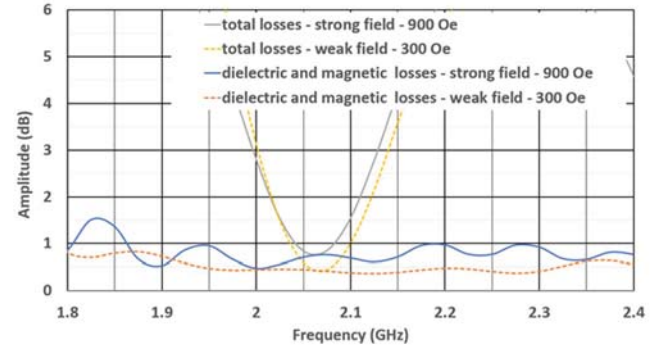


Fig. 5. Comparison of the losses (weak and strong field cases)

It should be reminded that the proposed antenna is designed to have a circular polarization. The Fig. 6 is comparing the axial ratio (AR) according to the frequency for the $\phi=0^\circ$ and $\theta=0^\circ$ position.

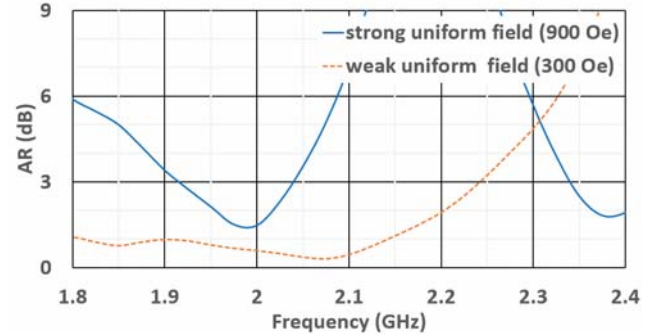


Fig. 6. Comparison of the axial ratio (weak and strong field cases)

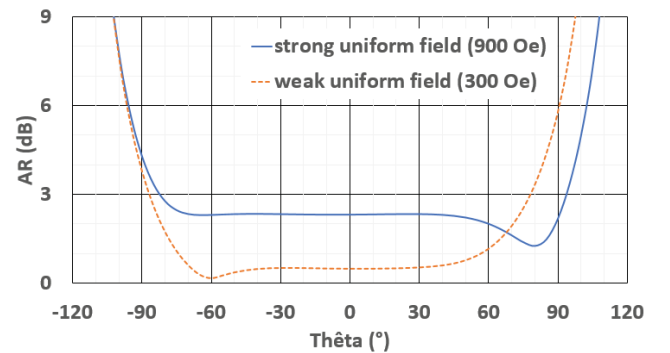


Fig. 7. Comparison of the axial ratio pattern at 2.025 GHz (weak and strong field cases)

The AR is remaining lower than -3dB on the whole matching bands for both cases. This axial ratio is also plotted

in the xOz plane according to the θ value at 2.025 GHz (Fig. 7). The circular polarization is better for the weak field case with a larger frequency coverage. Finally, the circular directivity is represented in Fig. 8 for the $\varphi=0^\circ$ and $\theta=0^\circ$ position at 2.025 GHz. It remains higher than 5dB for the two cases.

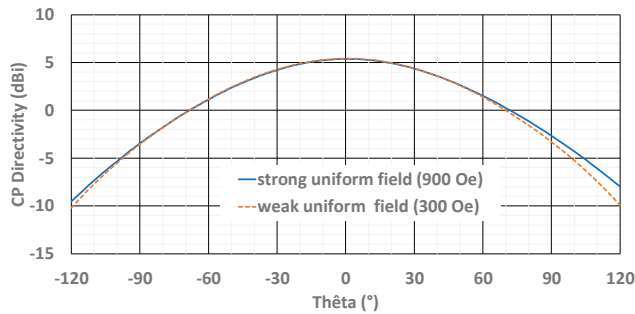


Fig. 8. Comparison of the realized gain ($\varphi=0^\circ$ and $\theta=0^\circ$) at 2.025 GHz (weak and strong field cases)

We demonstrated two operation modes for having circular polarized antennas. The strong field case is exhibiting highly reduced sizes with a larger impedance bandwidth while having an axial ratio lower than 3dB and a good realized gain. Therefore, we choose this case for the further study detailed in the next paragraph.

B. Magnetostatic and electromagnetic co-simulation

The last paragraph has presented two ideal cases since they are considering a uniform magnetic field within the ferrite. Before prototyping such an antenna, more investigations about this field need to be considered. In this framework, this paragraph is presenting the co-simulation of the previous patch antenna having a strong field operation by integrating a permanent magnet. This magnet is placed over the antenna top hat and its magnetic field strength of 1.35T is chosen to provide an internal magnetic field within all the ferrite not lower than 900 Oe to have a strong field operation. Fig. 9 is presenting the magnetic the real internal magnetic field within the ferrite of the patch antenna.

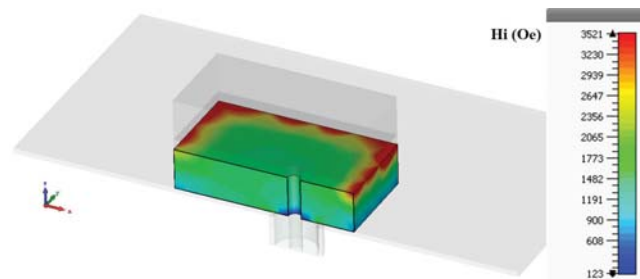


Fig. 9. Internal magnetic field within the ferrite

This figure shows that the internal magnetic field is not uniform according the three dimensions but it remains almost higher than 900 Oe. 2D cuts according the x- and y-directions in the middle of the ferrite height are plotted in Fig. 10.

In the middle level of the ferrite, the mean of H_i is equal to 1500 Oe, i.e. largely higher than 900 Oe. That involves an increase of the resonance frequency of the patch antenna compared to the uniform field case. To retrieve the initial working frequency of 2 GHz, lateral dimensions of the patch antenna must be increased. The optimized design of the antenna has dimensions of 17.7mmx17.7mmx4mm corresponding to $\lambda_0/8.5 \times \lambda_0/8.5 \times \lambda_0/37$ at 2 GHz.

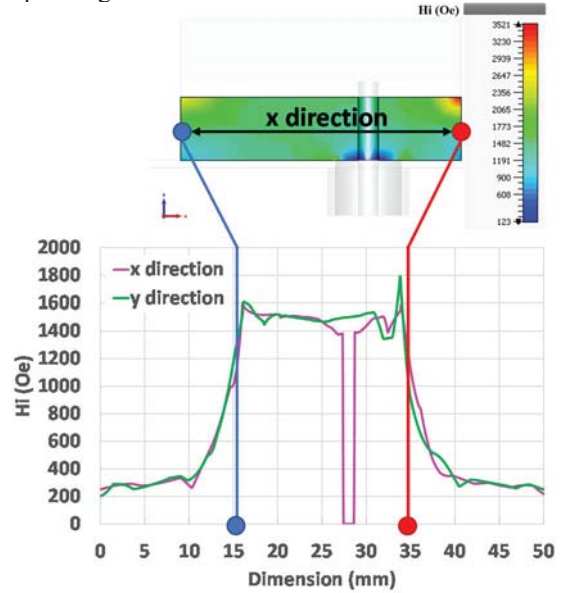


Fig. 10. Internal magnetic field in the middle of the ferrite.

This magnetic simulation is then integrated into the electromagnetic simulation to replace the previous uniform magnetic field of 900 Oe. The $|S_{11}|$ resulting of this co-simulation is plotted in Fig. 11 and compared with the ideal case, i.e. when the field is considered as uniform.

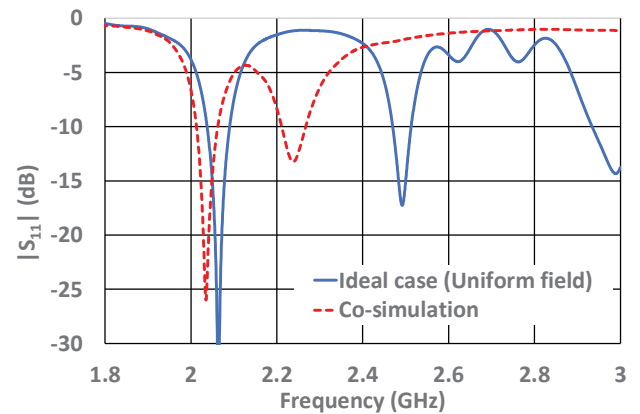


Fig. 11. $|S_{11}|$ parameters for the co-simulation and for the ideal case

The co-simulated antenna is well matched on an impedance bandwidth of 2.5%. The axial ratio is also investigated and is plotted in Fig. 12. The AR level is a little bit higher for the co-simulation case compared with the ideal one. However, it remains lower than -3dB on a larger angular coverage.

The RHCP realized gain is the same than the one presented in Fig. 8 since it is reaching a maximum of 5.25 dB at 2.025 GHz. Another critical point for miniature antennas is its efficiency. At this frequency the total efficiency, plotted in Fig. 13, is equal to 77%.

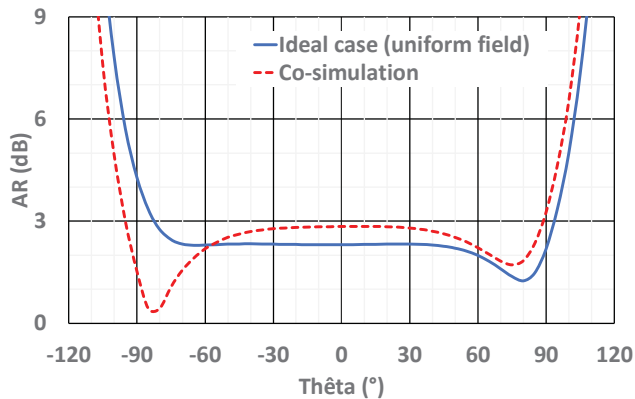


Fig. 12. Comparison of the axial ratio pattern at 2.025 GHz (ideal and co-simulation cases)

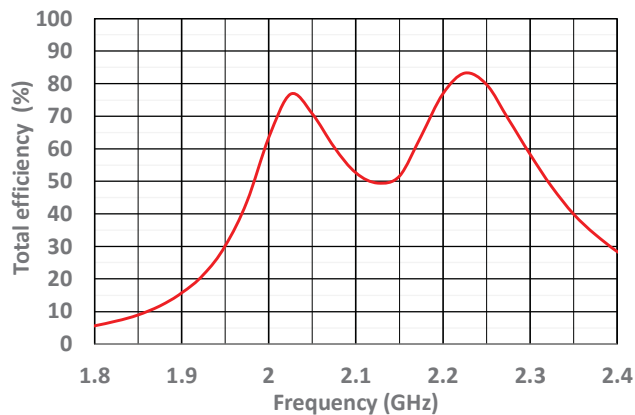


Fig. 13. Total efficiency of the co-simulated patch antenna

IV. CONCLUSION

We demonstrated how to miniaturize an antenna while having a circular polarization. A -3dB axial ratio on an average of 180° beam width is obtained with an antenna having highly reduced dimensions of $\lambda_0/8.5 \times \lambda_0/8.5 \times \lambda_0/37$ at 2 GHz. The circular polarization was achieved thanks to the use of a ferrite material meaning that no additional feeding network is required. A magnetostatic and electromagnetic co-simulation has been investigated for prototyping such an antenna. Both prototype and experimental measurements are in progress and will be presented at the conference.

ACKNOWLEDGMENT

The authors acknowledge the financial support through the Centre National d'Études Spatiales (CNES).

REFERENCES

- [1] C. Delaveaud, P. Leveque, B. Jecko, "New kind of microstrip antenna: the monopolar wire-patch antenna," *Electronics Letters*, vol.30, no.1, pp.1-2,6 Jan. 1994
- [2] L. Huitema, T. Reveyrand, J. L. Mattei, E. Arnaud, C. Decroze and T. Monediere, "Frequency Tunable Antenna Using a Magneto-Dielectric Material for DVB-H Application," in *IEEE Transactions on Antennas and Propagation*, vol. 61, no. 9, pp. 4456-4466, Sept. 2013
- [3] C.E.Fay et R.L.Comstock, «Operation of the Ferrite Circulator», *IEEE Trans.MTT-13*, Jan 1965, pp 15-27
- [4] Y. S. Wu and F. J. Rosenbaum, «Wideband operation of microstrip circulators», *IEEE Trans. Microwave Theory Tech.*, vol. MTT-22, pp. 849-856, Oct. 1974
- [5] J. B. Davies and P. Cohen, «Theoretical design of symmetrical junction stripline circulators», *IEEE Trans. Microwave Theory Tech.*, vol. MTT-11, pp. 506-512, Nov. 1963
- [6] N. Das and S. K. Chowdhury, "Microstrip rectangular resonators on ferrimagnetic substrates," in *Electronics Letters*, vol. 16, no. 21, pp. 817-818, October 9 1980. doi: 10.1049/el:19800581
- [7] J. S. Roy, P. Vaudon, A. Reineix, F. Jecko and B. Jecko, "Axially magnetized circular ferrite microstrip antenna," *IEEE Antennas and Propagation Society International Symposium 1992 Digest*, Chicago, IL, USA, 1992, pp. 2212-2215 vol.4. doi: 10.1109/APS.1992.221425
- [8] J. C. Batchelor, G. Classen and R. J. Langley, "Microstrip antennas on ferrites," *Tenth International Conference on Antennas and Propagation (Conf. Publ. No. 436)*, Edinburgh, 1997, pp. 30-33 vol.1. doi: 10.1049/cp:19970201
- [9] D. M. Pozar, "Radiation and scattering characteristics of microstrip antennas on normally biased ferrite substrates," in *IEEE Transactions on Antennas and Propagation*, vol. 40, no. 9, pp. 1084-1092, Sep 1992. doi: 10.1109/8.166534
- [10] D. Polder, «On the theory of ferromagnetic resonance», *Philos. Mag.*, vol. 40, 1949, p. 99-115
- [11] <http://www.exxelia.com/fr/groupe/a-propos/temex>
- [12] R. C. Hansen and M. Burke, "Antennas with magneto-dielectrics," *Microw. Opt. Tech. Lett.*, vol. 26, no. 2, pp. 75-78, Jul. 2000.